

Distribution of net community production and surface $p\text{CO}_2$ in the Scotia Sea, Antarctica, during austral spring 2001^a

JeongHee Shim ^{a,*}, Young Chul Kang ^b, Dongseon Kim ^a, Sang-Hwa Choi ^c

^a Ocean Climate and Environment Research Division, Korea Ocean Research and Development Institute, Ansan P.O. Box 29, Seoul 425-600, Korea

^b Polar Research Institute, Korea Ocean Research and Development Institute, Ansan P.O. Box 29, Seoul 425-600, Korea

^c Ocean Data and Information Department, Korea Ocean Research and Development Institute, Ansan P.O. Box 29, Seoul 425-600, Korea

Received 23 February 2004; received in revised form 3 November 2005; accepted 19 December 2005

Available online 2 March 2006

Abstract

Surface and water column measurements of $p\text{CO}_2$, alkalinity, and nutrients were made in the Scotia Sea in December 2001. From 54°S to 60°S along 52°W, $p\text{CO}_2$, TCO_2 , and nutrients in surface seawater increased southward. The $p\text{CO}_2$ concentration ranged from 370 μatm in the north to 420 μatm in the south and increased abruptly across the Polar and Scotia fronts by about 10–20 μatm . Net community production values from the preceding winter to the observation time were calculated at stations south of the Polar Front; values ranged from 1.0 to 1.2 mol m^{-2} and were comparable to other Southern Ocean measurements in summer, in or during an algal bloom. Processes affecting the surface $p\text{CO}_2$ distribution (e.g., thermodynamical change, air–sea exchange, biological production, and physical mixing) were evaluated from the preceding winter to the observation time at the stations. Seasonal warming increased surface $p\text{CO}_2$ at rates of 0.08–0.27 $\mu\text{atm day}^{-1}$; the highest values were observed at the station closest to the Polar Front. The air–sea exchange decreased surface $p\text{CO}_2$ at rates of -0.08 to -0.23 $\mu\text{atm day}^{-1}$, suggesting that the area around the study stations acted as a weak CO_2 source during the study period. The surface $p\text{CO}_2$ variation caused by biological production was -0.24 to -0.30 $\mu\text{atm day}^{-1}$ and was high south of the Scotia Front, where concentrations of chlorophyll *a*, biomass, and particulate Fe were relatively high. Physical mixing promoted an increase of 0.16–0.47 $\mu\text{atm day}^{-1}$ in surface $p\text{CO}_2$, a substantial contribution to total variation in $p\text{CO}_2$. This result contrasts with patterns in other Southern Ocean regions, where physical mixing was considered to be minimal or was ignored in previous studies. At station WS 8 in the Weddell–Scotia Confluence region, mixing was the dominant process of surface $p\text{CO}_2$ change during the study period, suggesting lateral and vertical transport of CO_2 -rich water masses from the Weddell Sea and the deep ocean.

© 2006 Elsevier B.V. All rights reserved.

Keywords: Net community production; CO_2 flux; Carbon cycle; Scotia Sea; Weddell–Scotia Confluence; Antarctica

1. Introduction

The observed increase in atmospheric concentrations of carbon dioxide (Keeling and Whorf, 1994) has

spurred considerable interest among researchers and has altered the global carbon cycle (Sarmiento, 1993; Tans et al., 1990; Sarmiento et al., 1992). Oceans are thought to have taken up $1.7\text{--}1.9\pm 0.6$ PgC year^{-1} from anthropogenic sources during the 1980s and 1990s (IPCC, 2001). Of this amount, more than 20% has been taken up by the Southern Ocean (south of 50°S), though

* Corresponding author.

E-mail address: jhshim@kordi.re.kr (J. Shim).

the area accounts for less than 10.2% of global oceans (Takahashi et al., 2002).

From the late 1980s to the early 1990s, several surveys examined atmospheric CO₂ uptake by the Southern Ocean (Metzl et al., 1991; Poisson et al., 1993; Takahashi et al., 1993; Bellerby et al., 1995; Hoppema et al., 1995; Robertson and Watson, 1995; Bakker et al., 1997; Rubin et al., 1998). Surface *p*CO₂ data from the Southern Ocean have shown large spatial and temporal variability. Whether the Southern Ocean as a whole serves as a net sink or net source of atmospheric CO₂ is still being debated, highlighting the complexity of carbon chemistry in the Southern Ocean and lack of surface water CO₂ data, notably in autumn and winter.

Net community production (NCP), which is the difference between primary production and respiration by all auto- and heterotrophic organisms present in a water column (Codispoti et al., 1986; Minas et al., 1986), has been used in high latitude areas to quantify the net CO₂ consumed biologically in the euphotic layer. This method can determine the total inorganic carbon and nutrient deficits in the upper mixed layer with reference to concentrations in the temperature minimum (*T*_{min}) layer, which represents remnants of the winter mixed layer. Global net community production was also

estimated using biogeochemical mass balances of O₂, NO₃⁻, PO₄²⁻, and total dissolved inorganic carbon in the mixed layer (Louanchi and Najjar, 2000; Lee, 2001). Especially in the Southern Ocean (south of 40°S), values of net community production ranged from 0.73 to 3.48 Gt C year⁻¹ (Lee, 2001; references therein). Detailed quantification of NCP over the Southern Ocean, composed of a “mosaic” of subsystems (Tréguer and Jacques, 1992; Álvarez et al., 2002; Castro et al., 2002), is a key factor in determining the role of this ocean in the global carbon cycle.

The Weddell Sea is traditionally regarded as one of the main locations for bottom-water formation around Antarctica, due to enhanced atmosphere–ice–ocean interaction (Gill, 1973; Carmack, 1977). The sea is concurrently seen as a CO₂ source, owing to upwelling of warm deep water with high CO₂ concentrations (Weiss et al., 1979; Takahashi et al., 1993). Therefore, many studies have focused on carbon chemistry and water circulation of the Weddell Sea (Fahrbach et al., 1995; Hoppema et al., 1995, 1998a,b; Hoppema and Goeyens, 1999; Hoppema et al., 2002; Stoll et al., 2002). The Scotia Sea is a rather small region in the Southwest Atlantic, which ‘provides a pathway for recently ventilated waters from the Weddell Sea into the

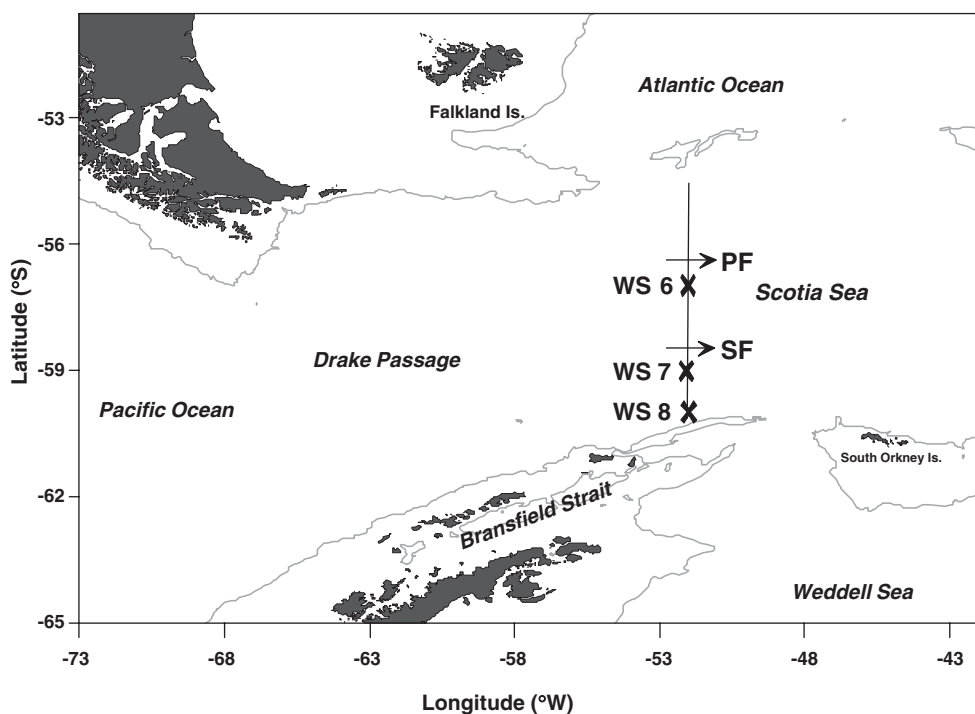


Fig. 1. Map showing the study area. The solid line shows the surface water observations and the hydrographic transect along 52°W. The sites for vertical observations are indicated by crosses (x). The gray line shows the 1000 m depth contour and the black arrows indicate the location of fronts: PF (Polar Front) and SF (Scotia Front).

deep western boundary current of the South Atlantic' (Fig. 1; Orsi et al., 1999; Naveira Garabato et al., 2002). Between the Weddell and Scotia Seas, there is 'a quasi-zonal band of eastward flow and weak stratification called the Weddell–Scotia Confluence' (Whitworth et al., 1994). The Weddell–Scotia Confluence serves as a specific zone of interaction for Weddell, Scotia, and Bellingshausen Sea waters, as well as for local thermodynamic processes in the southern Scotia Sea (Patterson and Sievers, 1980). Thus, the Scotia Sea and the Weddell–Scotia Confluence are important for our understanding of carbon chemistry in areas to which Weddell Sea water, which has been freshly ventilated and is rich in inorganic carbon, is neighbored.

In this study, we present data from the 15th Korean Antarctic Research Program (KARP) research cruise, which was conducted during the spring of 2001/2002. This study aimed (i) to evaluate spatial variations in surface water carbon dioxide, (ii) to estimate NCP in the mixed layer, and (iii) to quantitatively evaluate processes affecting $p\text{CO}_2$ variation from winter to spring in the Scotia Sea and in the Weddell–Scotia Confluence.

2. Materials and methods

Observations of partial pressure of carbon dioxide ($p\text{CO}_2$), total alkalinity (TA), temperature, salinity, dissolved oxygen, and nutrients in surface waters were carried out aboard the *R/V Yuzhmorgeologia* in the latitudes of 54–60°S along 52°W longitude during the 15th KARP research cruise from 20 November to 31 December 2001 (Fig. 1). Samples consisted of surface water pumped continuously from a depth of ~5 m and deep waters collected with Niskin bottles mounted on a conductivity–temperature–depth (CTD) rosette sampler. Continuous measurements of $p\text{CO}_2$, temperature, and salinity were made for surface waters; samples for TA and nutrients were taken every hour from surface water. Deep waters for vertical profiles of TA, dissolved oxygen, and nutrients were obtained at three stations (WS 6, 7, and 8) located at 57, 59, and 60°S along 52°W longitude, respectively. At each station, hydrographic profiles of temperature, salinity, and density were also taken. Fig. 1 shows the track for surface measurements and the locations of the three stations for vertical profiles.

The $p\text{CO}_2$ in the surface water (every minute) and the atmosphere (every hour) was determined using a flowing $p\text{CO}_2$ system and an equilibrator similar to those designed by Wanninkhof and Thoning (1993) and Weiss (1981), respectively. The fraction of CO_2 in the equilibrated air sample was measured with a Li-COR model 6262 infrared

CO_2 and H_2O analyzer (Goyet and Peltzer, 1993). The samples were measured wet, and the signal was internally corrected to dry air at 1-atm pressure using the in situ measurements from the Li-COR water channel and connected pressure sensor. The system was calibrated using two standard gases, 270 ± 3.5 and 540 ± 4.3 ppm CO_2 in air (Airgas Inc., USA).

The alkalinity titration system was similar to that described by Millero et al. (1993). The titration system consisted of a titrator (Metrohm, model 665 Dosimat) and a pH meter (Orion, model 720 A) controlled by a personal computer. The plexiglass water-jacketed cells used during the cruise were similar to those used by Bradshaw and Brewer (1988), except that a larger volume (about 200 cm^3) was used in our study for greater precision. Seawater samples were titrated by adding hydrochloric acid (HCl) to the carbonic acid end point. The temperature of both the acid titrant in a water-jacketed burette and the seawater sample in a water-jacketed cell were controlled to a constant temperature of 25.0 ± 0.5 °C by means of a constant temperature bath (Jeio Tech, model WBC-1520). The consistency of the measurements was checked for each cast of samples using low-nutrient surface seawater and standard reference materials (SRM) provided by Prof. F. Millero. The SRM was made in the laboratory of Prof. F. Millero with TA and TCO_2 values at 2329.11 ± 1.521 $\mu\text{mol kg}^{-1}$ and 2025.85 ± 1.430 $\mu\text{mol kg}^{-1}$ (Batch #9), respectively. We measured the SRM once a day for surface water measurement and once at each station for hydrographic measurement. Analytical precision (± 1 s) was estimated to be ± 3.5 $\mu\text{mol kg}^{-1}$, and differences in our analytical results for the SRM from its certified value were 3.5 ± 2.0 $\mu\text{mol kg}^{-1}$ during the cruise. Total carbon dioxide (TCO_2) in surface seawater was automatically calculated by the TA system using the TA and pH, measured with the TA system; calculations used the solubility of CO_2 in seawater given by Weiss (1974), the dissociation constants of carbonic acid given by Roy et al. (1993), and the dissociation constant of boric acid given by Dickson (1990).

Joint Global Ocean Flux Study (JGOFS) protocols (Knap et al., 1996) were used for sampling, measurement, and standardization of nutrients and dissolved oxygen. Concentrations of nutrients (nitrate+nitrite, phosphate, and silicate) were determined with a continuous-flow analytical system (Lachat, model QuickChem AE), which was calibrated using brine standard solutions (Wako Pure Chemical Industries, CSK Standard Solutions). The repeatability of the analyses was checked using seawater samples taken at depths of about 3000 m. Oxygen samples were analyzed

by the Winkler method using an autoburette (Metrohm, model 775 Dosimat). The duplicate values were within $0.4 \mu\text{mol kg}^{-1}$ of seawater. Apparent oxygen utilization (AOU) was calculated as the difference between the observed concentration and the equilibrium concentration in the atmosphere (Weiss, 1970) for the potential seawater temperature.

3. Results

3.1. Vertical section of hydrographic properties

The study area is situated within the western South Atlantic sector of the Antarctic Circumpolar Current (ACC; Fig. 1). The cruise track, from 54°S to 60°S along 52°W , extended from the western South Atlantic to the Scotia Sea and crossed two fronts: the Polar Front and the Scotia Front. The Polar Front is identified by the northern terminus of the subsurface temperature minimum (T_{min}) layer, which is bounded by the 2°C isotherm in the 100–300 m layer in summer (Belkin and Gordon, 1996; references therein). The Scotia Front, which is the northern boundary of the Weddell–Scotia Confluence, is a distinct subsurface front, marked by a maximum thermal gradient in the T_{max} core layer (200–700 m) of the Circumpolar Deep Water (CDW). Analysis of many sections across the Scotia Front shows that the 1°C isotherm in the 300–500 m layer is a fair indicator of the Scotia Front axis (Gordon et al., 1977; Belkin and Gordon, 1996). South of the Scotia Front, the Weddell–Scotia Confluence separates the waters of the Weddell and Scotia Seas.

Fig. 2 shows the vertical section of temperature, salinity, and density in the upper 500 m from 54°S to 60°S along 52°W in December 2001. The Antarctic Polar Front separates the Antarctic Polar Frontal Zone from the Antarctic Zone. The second front in our study region, the Scotia Front, separates the Antarctic Zone from the Weddell–Scotia Confluence. In December 2001, the Polar Front and the Scotia Front were located around 56.5°S and 58.0°S , respectively. The subsurface T_{min} layer, which is colder than 2°C , extended south from 56.5°S , and the 1°C isotherm was close to 500 m at 58.0°S .

Temperatures in surface waters north of the Polar Front decreased gradually from the surface to a depth, as compared to temperatures south of the front, where a subsurface T_{min} layer existed around depths of 100–250 m (Fig. 2a). The area north of the Polar Front showed a thermocline at a depth of about 100 m. Surface salinity north of the Polar Front was generally constant over 500 m depth, as compared to surface

salinity south of the front, where salinity changed significantly with depth, and a strong halocline was located at 200–400 m depth (Fig. 2b). Low salinity in the surface layer south of the Polar Front might be the effect of meltwater in situ and/or from the upstream. Distributions of potential density (σ_t) south of the Polar Front were parallel to salinity distributions. In contrast, in the northern region, the density change with depth was similar to that of temperature. These results confirm the conclusions by Pollard et al. (2002) for the Indian sector of the Southern Ocean. A pycnocline developed in the subsurface layer both north and south of the Polar Front. Only a small meridional gradient of σ_t in surface waters was found near the Polar Front, as salinity counteracted the effect of temperature (Fig. 2c).

3.2. Longitudinal distribution of surface properties

Fig. 3 shows meridional distributions of temperature, salinity, $p\text{CO}_2$, TA, TCO_2 , and nutrients (nitrate + nitrite, phosphate, and silicate) in surface waters from 54°S to 60°S , along 52.0°W , in December 2001. Values of TA, TCO_2 , and nutrients were normalized to a constant salinity of $S=34$ to correct for melting and precipitation/evaporation influences.

Temperature and salinity in surface waters showed abrupt variations at the fronts, as shown by the arrows in Fig. 3a. The surface temperature exhibited a significant decrease (from 4.5 to 1°C within only 0.5° of latitude) across the Polar Front. South of the PF, temperature gradually decreased southward. A gradual southward decrease occurred with nearly constant values (1 – 0.5°C), except for some fluctuations near the Scotia Front. Over the whole transect, salinity ranged from 33.7 to 34.3. Across the Polar Front to the south, salinity decreased below 34; across the Scotia Front, salinity increased to about 34.

Surface water $p\text{CO}_2$ ranged from 370 to $420 \mu\text{atm}$ and was supersaturated relative to the atmosphere (368 – $374 \mu\text{atm}$) by up to $\sim 50 \mu\text{atm}$ (Fig. 3b). In particular, $p\text{CO}_2$ showed abrupt southward increases when crossing the two fronts; values increased by about 10 and $20 \mu\text{atm}$ near the Polar and Scotia Fronts, respectively. Variation of $p\text{CO}_2$ near the fronts corresponded to variations in TCO_2 and nutrient concentrations and was opposite to the trend in temperature. The large $p\text{CO}_2$ gradient corresponded to the substantial gradient in TCO_2 concentration. The TA and TCO_2 values, normalized at $S=34$, varied from 2320 to $2380 \mu\text{mol kg}^{-1}$ and from 2150 to $2250 \mu\text{mol kg}^{-1}$, respectively, and increased to the south (Fig. 3c).

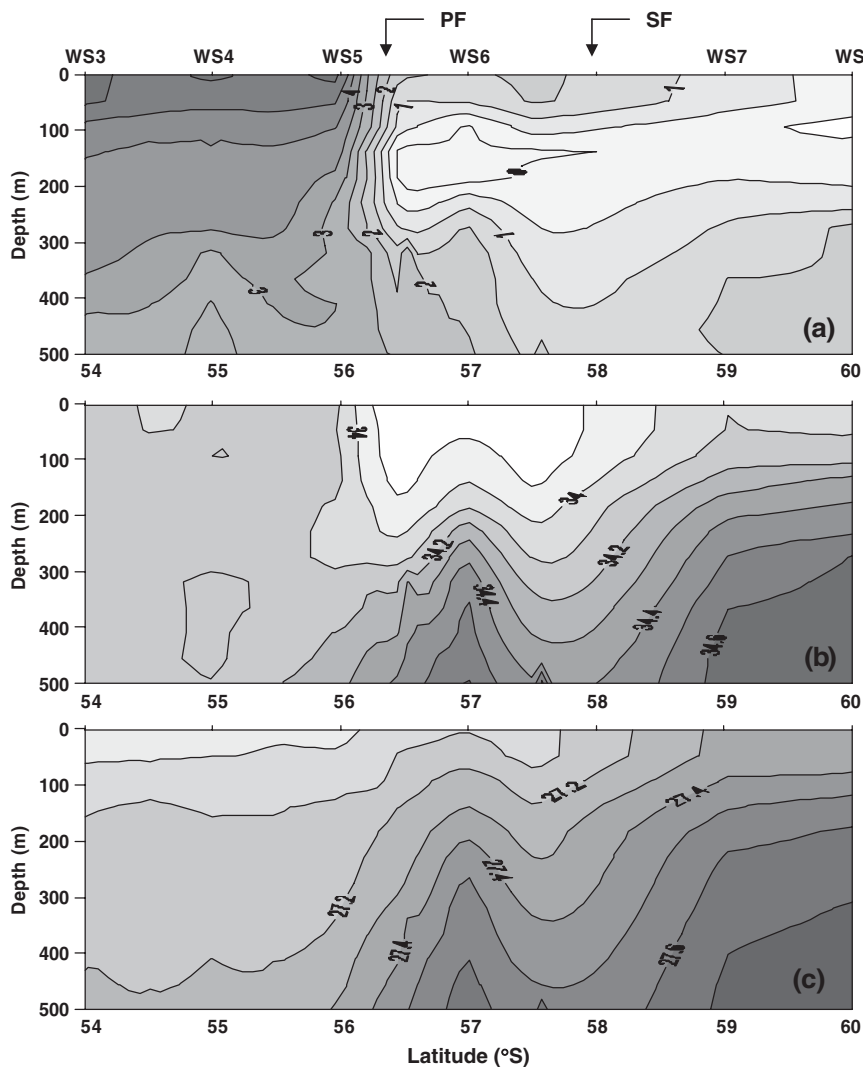


Fig. 2. Vertical sections of temperature ($^{\circ}\text{C}$) (a), salinity (b) and potential density (σ_t) (c) along 52°W in December 2001. The arrows indicate the location of fronts: PF (Polar Front) and SF (Scotia Front).

When crossing the fronts, TA and TCO_2 values showed southward increases by about 20 and $50 \mu\text{mol kg}^{-1}$, respectively. Increases in $p\text{CO}_2$ and TCO_2 were more dramatic near the Scotia Front than near the Polar Front, while the temperature change was greater near the Polar Front.

Surface concentrations of nitrate+nitrite, phosphate, and silicate were normalized to a salinity value of 34 and increased to the south, especially at the two fronts (Fig. 3d). Increases of nitrate+nitrite, phosphate, and silicate over the track were about 10, 0.5, and $60 \mu\text{mol kg}^{-1}$, respectively. Across the Scotia Front, silicate increased by about $40 \mu\text{mol kg}^{-1}$ or twice the increase found in the Polar Front. The nitrate+nitrite and phosphate concentrations increased at both the Polar and Scotia

Fronts with the same rate. This suggests that compared to water properties north of the Scotia Front, those south of Scotia Front may be affected more from CO_2 and silicate-rich water by upwelling, diffusion and physical transport from the deep water and/or neighbored water masses.

3.3. Vertical distribution south of the Polar Front

Fig. 4 illustrates the results of vertical observations in the upper water column at stations WS 6, 7, and 8 in December 2001. At all three stations, located south of Polar Front, a temperature-minimum (T_{min}) layer was observed in the sub-surface at water depths of about 100–250 m (Fig. 4a). This layer is a remnant of the

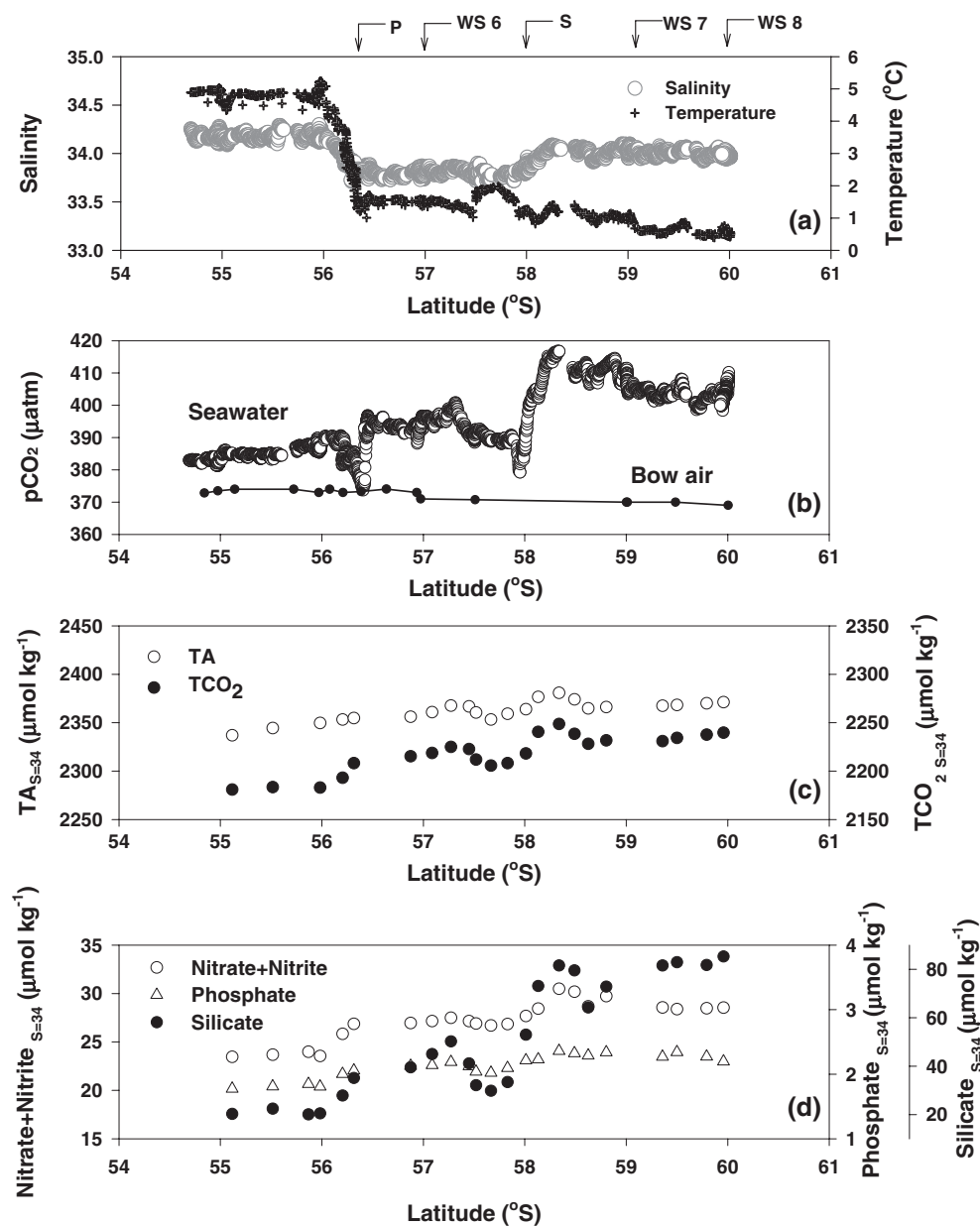


Fig. 3. Meridional distributions of salinity and temperature ($^{\circ}\text{C}$) (a), $p\text{CO}_2$ (μatm) (b), total alkalinity and total inorganic carbon ($\mu\text{mol kg}^{-1}$) normalized to $S=34$ (c) and nitrate+nitrite, phosphate and silicate ($\mu\text{mol kg}^{-1}$) normalized to $S=34$ (d) in surface waters along 52°W in December 1–2, 2001. Arrows show the locations of fronts: P, Polar Front; S, Scotia Front.

winter surface layer, and its properties can be used as proxies for those in the winter mixed layer (Jennings et al., 1984; Minas and Minas, 1992; Ishii et al., 1998; Rubin et al., 1998; Pondaven et al., 2000). Overlying the cold T_{min} layer, a surface layer with relatively warm and less saline water was observed. At station WS 6, temperature and salinity changed gradually from below 50 m to the T_{min} depth, developing a shallow pycnocline. In contrast, at stations WS 7 and WS 8,

approximately constant temperatures were observed above about 80 m and changed sharply from those of the T_{min} layer. Salinity values at stations WS 7 and 8 were similar within the mixed layer and higher than those at station WS 6 at the same depth; thus, the water at stations WS 7 and 8 was denser (Fig. 4b and c). Above the T_{min} layer, AOU values were negative or low (less than $8 \mu\text{mol kg}^{-1}$) and constant with depth at all WS stations (Fig. 4d). Below the T_{min} layer, the AOU

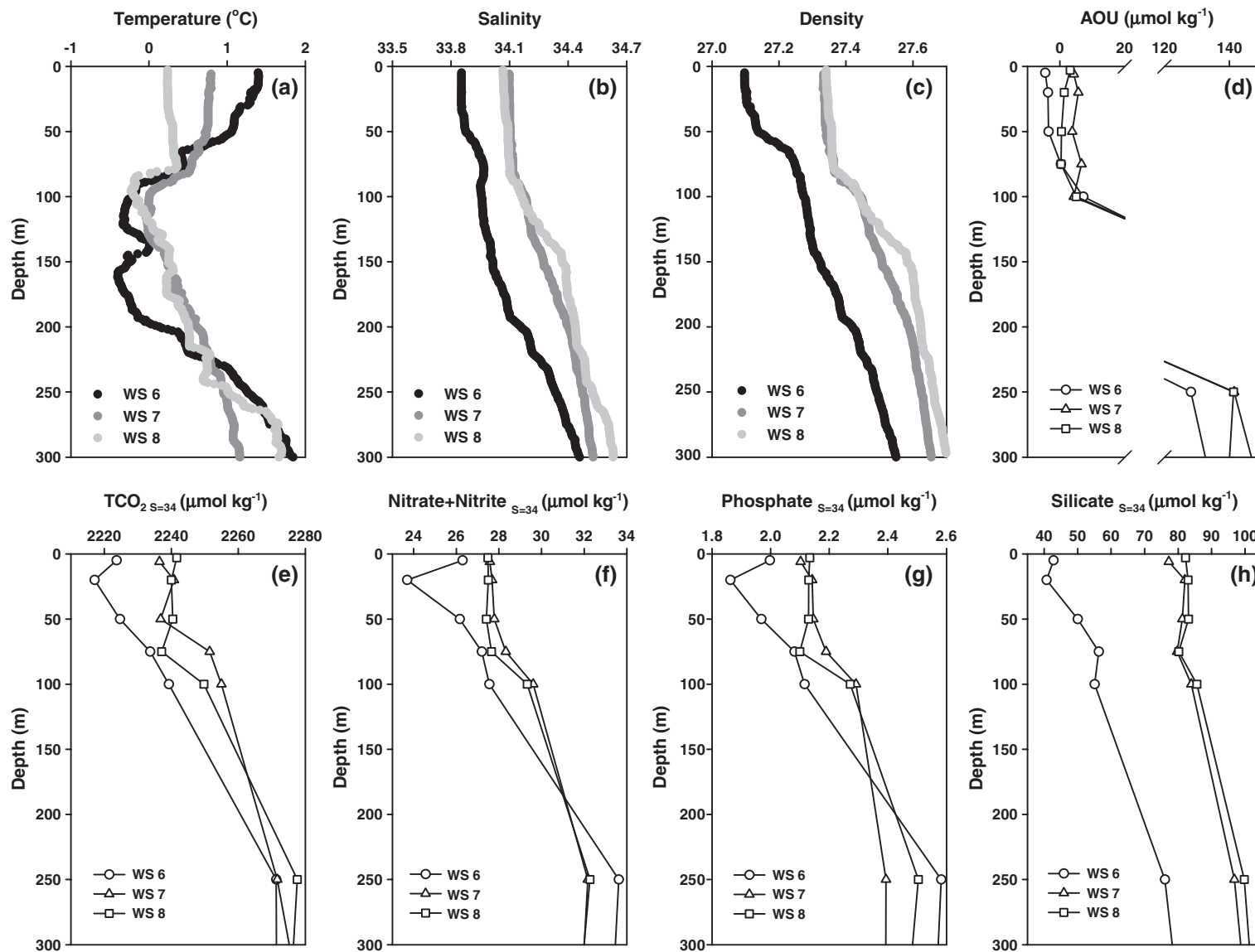


Fig. 4. Vertical profiles of temperature ($^{\circ}\text{C}$) (a), salinity (b), potential density (σ_t) (c), AOU ($\mu\text{mol kg}^{-1}$) (d), total inorganic carbon ($\mu\text{mol kg}^{-1}$) normalized to $S=34$ (e), nitrate+nitrite ($\mu\text{mol kg}^{-1}$) normalized to $S=34$ (f), phosphate ($\mu\text{mol kg}^{-1}$) normalized to $S=34$ (g) and silicate ($\mu\text{mol kg}^{-1}$) normalized to $S=34$ (h) at 57°S (WS 6), 59°S (WS 7) and 60°S (WS 8) along 52°W in December 2001.

Table 1

Observed concentrations in the T_{\min} layer and deficits in the water column above the T_{\min} layer at each station south of the Polar Front at 52°W

Station (Location)	Winter concentration ($\mu\text{mol kg}^{-1}$)						Integrated deficits (mmol m^{-2})				NCP by N deficit (mol C m^{-2})
	Temperature (°C)	TCO_2	NO_{3+2}^-	PO_4^{3-}	SiO_4^-	$p\text{CO}_2$ (μatm)	TCO_2	NO_{3+2}^-	PO_4^{3-}	SiO_4^-	
WS 6 (57°S, 52°W)	-0.311	2239	27.5	2.12	55.0	379.9	1305	154	12.5	600	1.0
WS 7 (59°S, 52°W)	-0.006	2255	29.6	2.29	83.9	413.9	1179	167	13.6	259	1.1
WS 8 (60°S, 52°W)	-0.233	2250	29.3	2.27	85.6	401.3	1024	181	20.1	251	1.2

increased to values of more than $120 \mu\text{mol kg}^{-1}$. These results suggest that the balance of remineralization of organic matter and primary production was minimal within the mixed layer, and/or the air–sea gas exchange was active from winter to spring.

Distributions of salinity-normalized concentrations of TCO_2 and nutrients showed an increase with depth; all values at stations WS 7 and 8 were much higher than those at WS 6 at the same depths, as with the distribution of salinity (Fig. 4e–h). TCO_2 values above the T_{\min} layer ranged from 2230 to 2255 $\mu\text{mol kg}^{-1}$ at stations WS 7 and 8, whereas the values ranged from 2210 to 2240 $\mu\text{mol kg}^{-1}$ at WS 6. The TCO_2 values of the T_{\min} layer were also higher at WS 7 and 8 than at WS 6 (Table 1). Nutrients also were higher at WS 7 and 8 than at WS 6. In particular, silicate at WS 7 and 8 was about double that of WS 6. Above the T_{\min} layer, the concentration of the winter surface, a decrease of TCO_2 occurred at all three stations. These decreases above the T_{\min} layer were also repeated in distributions of nitrate + nitrite, phosphate, and silicate at each station, and the decrease pattern of nutrients was very similar to that of TCO_2 within a station (Fig. 4). This suggests that nutrient variation in the water column correlated with variation in TCO_2 ; thus, biological production may account for the decrease in TCO_2 and nutrients in the mixed layer from winter to the study period.

4. Discussion

4.1. Estimate of net community production

Net community production (NCP), the net amount of organic carbon produced, has been estimated from in situ observations of water column changes in oxygen, nitrate + nitrite (Jennings et al., 1984), TCO_2 (Weiss et al., 1979; Karl et al., 1991), and $p\text{CO}_2$ (Robertson and Watson, 1993; Bates et al., 1998 and references therein). Recently, in high-latitude areas, researchers have measured NCP not only during the time of observation,

but also from the difference between winter values and values at the time of observation in order to understand seasonal variation in biological production and CO_2 sink functions (Ishii et al., 1998; Sweeney et al., 2000a; Ishii et al., 2002; Midorikawa et al., 2002; Murata et al., 2002; Tsurushima et al., 2002). Because severe weather and sea state conditions limit direct winter measurements in the polar regions, researchers have estimated NCP from winter to the observation time by using vertically integrated deficits of TCO_2 and/or nitrate referenced with concentrations in the remnant T_{\min} layer in spring or summer. We observed the subsurface T_{\min} layer at stations WS 6, 7, and 8, which had temperatures near the freezing point and negative or low AOU values (Fig. 4d). These conditions suggest good preservation of properties of the winter mixed layer in the T_{\min} layer. Thus, concentrations of TCO_2 and nutrients in the T_{\min} layer could be considered directly representative of concentrations in the winter mixed layer, without significant remineralization of organic matter. The values of carbon parameters and nutrients at 100 m depth, the upper limit of the T_{\min} layer at the three WS stations, were assumed to be winter surface concentrations. Winter concentrations of TCO_2 , nutrients, and $p\text{CO}_2$ at the WS stations are listed in Table 1. Of the winter concentrations, $p\text{CO}_2$ was calculated from TA and TCO_2 using the program of Lewis and Wallace (1998). In this program, TA and TCO_2 values at 100 m depth were used as input parameters in addition to temperature, salinity, concentrations of phosphate and silicate at 100 m depth, and the Hanssen and Mehrbach constants refitted by Dickson and Millero (1987) used for the seawater CO_2 system. The uncertainty in these calculations of $p\text{CO}_2$, based on analytical errors in TA, TCO_2 , and other parameters, was about $\pm 5\%$.

Winter concentrations of TCO_2 and nutrients increased southward across the Scotia Front; the values at WS 7 and 8 were much higher than those at WS 6. Concentrations of TCO_2 and silicate at WS 7 and 8 exceeded those at WS 6 by about 10 and 30 $\mu\text{mol kg}^{-1}$,

respectively. Calculated winter $p\text{CO}_2$ values ranged from 380 μatm at WS 6 to >400 μatm at WS 7 and 8.

In the Southern Ocean south of Australia, Ishii et al. (2002) reported that the TCO_2 of the winter mixed layer in the seasonal ice zone is constant over a wide area (2182–2184 $\mu\text{mol kg}^{-1}$). They also suggested that the normalized TCO_2 in the mixed layer in late winter shows little spatial variation over most of the seasonal ice zone in the Southern Ocean, and that zonal advection is not problematic in calculating the TCO_2 deficit in the summer surface layer of this zone. Compared with these results, our winter TCO_2 values are somewhat higher and have a wider spatial variation (2239–2255 $\mu\text{mol kg}^{-1}$). Gordon (1971) noted that locally high $p\text{CO}_2$ and nutrient values had been observed along the Weddell–Scotia Confluence, where dynamics of currents and interactions with topography appear to cause deep-water upwelling. In addition, von Gyldenfeldt et al. (2002) reported that the Scotia Sea is supplied by water from the Powell Basin, located in the north-western Weddell Sea. Thus, water south of the Scotia Front was supersaturated with CO_2 and silicate in late winter, suggesting that CO_2 - and silicate-rich water may have been transported into the mixed layer by upwelling, deep mixing, and lateral advection from the deep ocean and the adjacent Weddell Sea and/or may have been produced by remineralization of organic matter. The properties of the mixed layer in our study area varied in relation to the degree of upwelling and convection from deep and southern part of water masses, especially with respect to carbon and silicate components.

Deficits in TCO_2 , nitrate+nitrite, phosphate, and silicate above the T_{min} layer of about 100 m water depth at the WS stations were computed for each hydrographic station. In general, deficit ratios of TCO_2 and nutrients in the surface layer depend on the uptake by phytoplankton and subsequent remineralization by the plankton community. Deficits in TCO_2 , nitrate+nitrite, phosphate, and silicate ranged from 1023–1305, 154–180, 12.6–20.1, and 251–600 mmol m^{-2} , respectively. The ratios of $\Delta\text{C}/\Delta\text{N}$, $\Delta\text{C}/\Delta\text{P}$, $\Delta\text{Si}/\Delta\text{C}$, and $\Delta\text{N}/\Delta\text{P}$, calculated from the slopes in Fig. 5, were 5.7, 85.2, 0.53, and 12.7, respectively; the overall ratio of Si/C/N/P was 49:85:13:1. This ratio was lower for C and N than the traditional Redfield ratio of 106:16:1 (Redfield et al., 1963) but higher than that for the Australian sector of the Southern Ocean (39:54:8.7:1; Ishii et al., 2002). Ishii et al. (1998) reported that the C/N/P ratio of composite plots in marginal ice zones was 58:9.2:1 off Lützow-Holm Bay (38°E), off Casey Bay (48°E), in Prydz Bay (75°E), and in the seasonal ice zone between 59°E and

97°E. They concluded that these deficit ratios would have little spatial variation over the Indian Ocean sector and the Australian sector, although some exceptions could occur in offshore regions.

Nutrient uptake ratios by phytoplankton are thought to change with algal species as well as with their environmental and physiological conditions. Arrigo et al. (1999) reported that drawdown of both carbon dioxide (CO_2) and nitrate per mole of phosphate, as well as the rate of new production by diatoms, are much lower than those measured for *Phaeosystis antarctica*. In the Ross Sea, deficit ratios of C/P and C/N for diatom-dominated blooms were 80.5 and 7.8, while those for a bloom dominated by *P. antarctica* were 134 and 7.2 (Sweeney et al., 2000b). Sweeney et al. (2000b) noted that species dependence in C/P ratios, and the relative constancy of C/N ratios, make N a better proxy of biological CO_2 utilization than P. Therefore, to calculate NCP at the WS stations, we used the nitrate + nitrite deficits (ΔN) and applied the Redfield ratio of 6.6 for converting to the carbon deficit, rather than the TCO_2 deficits and thus the deficit ratio of C/N (5.7 at Fig. 5a), which have to be corrected for air–sea exchange when used as a proxy for NCP calculations. Uncertainty of NCP, based on in situ and winter nutrient concentrations and on the Redfield ratio, is about $\pm 8.5\%$.

The NCP based on ΔN ranged from 1.0 to 1.2 mol C m^{-2} along the WS stations (Table 1). This value is comparable to those from other Antarctic regions, though it was measured in spring rather than in summer (Table 2). Except for extremes in the Ross Sea, the NCP from winter to summer ranged from 0.3 to 4.0 mol m^{-2} in the Southern Ocean (Jennings et al., 1984; Minas and Minas, 1992; Ishii et al., 1998; Rubin et al., 1998). Along the WS stations, NCP showed a southward increase and the highest values at WS 8. This result is in fair agreement with the results for chlorophyll *a*, carbon biomass of the microbial community, and particulate Fe in the upper layer during the research cruise (Hyun and Yang, 2003; Kang et al., 2002; Kim, 2003). The chlorophyll *a* concentration was about 0.7–0.9 $\mu\text{g l}^{-1}$ at WS 7 and 8 and showed vertically homogeneous distributions from the surface to 50 m depth. In contrast, the chlorophyll *a* concentration at WS 6 was about 0.2–0.4 $\mu\text{g l}^{-1}$, half of that at WS 7 and 8 (Kang et al., 2002). The carbon biomass of the microbial community was >3000 mg C m^{-2} at WS 7 and 8, whereas the concentration at WS 6 was about 2000 mg C m^{-2} (Hyun and Yang, 2003). The concentration of particulate Fe, which is a limiting factor of primary productivity in the Southern Ocean (de Baar et al.,

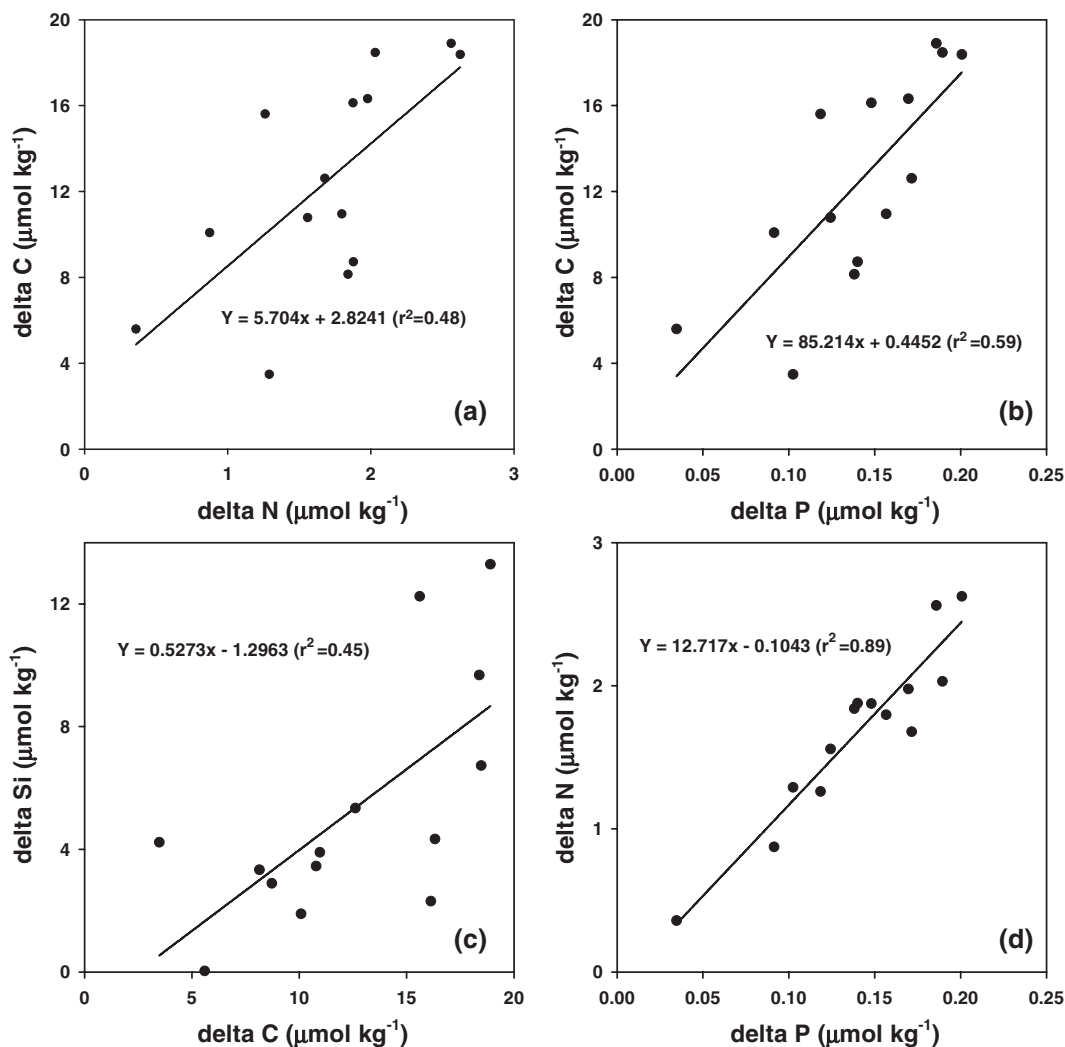


Fig. 5. Composite plots of the deficit of total inorganic carbon against the deficit of nitrate+nitrite (a), the deficit of total inorganic carbon against the deficit of phosphate (b), the deficit of silicate against the deficit of total inorganic carbon (c) and the deficit of nitrate+nitrite against the deficit of phosphate (d) in the upper water column above the subsurface temperature minimum (T_{min}) layer at a total of 3 hydrographic stations (WS 6, 7 and 8) south of Polar Front along 52°W .

1990, 1995; Martin et al., 1990), was about 16–47 nM at stations WS 7 and 8, and neared zero (0.5 nM) at WS 6 (Kim, 2003). The high chlorophyll *a* concentration, carbon biomass of the microbial community, and particulate Fe at stations WS 7 and 8 suggest that biological production was more active at these stations than at WS 6, as in the results of NCP based on nitrate deficits.

Although requiring correction for the variation due to the air–sea exchange, the deficits in TCO_2 ranged within much similar values (1.0–1.3 mol C m^{-2}) to the results of NCP calculated from nitrate deficits (Table 1). However, WS 6 showed a high value compared to WS 7 and 8, where the NCP and other parameters were high.

This result suggests that the nitrate deficit is a good tool for calculating the NCP, while other parameters, such as TCO_2 and phosphate, need correction for gas exchange and for species dependence of biological absorption, respectively.

4.2. A simple budget of surface $p\text{CO}_2$

The $p\text{CO}_2$ in the upper mixed layer is controlled by the following processes: thermodynamical change, air–sea exchange, biological activity, and mixing processes (Chipman et al., 1993). To assess processes governing variability in surface $p\text{CO}_2$ from winter to the observation time for WS stations, a simple and modified

Table 2
Comparison of seasonally integrated net community production (NCP)

Location	Period	NCP (mol m ⁻²)	References
Weddell Sea (60°S, 0°)	Winter–January (60–90 days)	1.7	Jennings et al. (1984)
Southern Ocean, Indian sector (48°–62°S, 65°E)	Winter–February/ March	2.5	Minas and Minas (1992)
Southern Ocean, Indian and Pacific sector (63°–69°S, 30°–150°E)	Winter–February/ March	0.8–4.0	Ishii et al. (1998)
Southern Ocean, Pacific sector (67°–69.7°S, 110°–170.6°E)	September/October– February/March (~120 days)	0.8–2.9	Rubin et al. (1998)
Ross Sea (74.3°–78°S, 163°–187°E)	October–January/ February	1.2–10.8	Sweeney et al. (2000a)
Southern Ocean, Pacific sector (64°–65.5°S, 140°E)	Winter–December/ January	0.3–2.5	Ishii et al. (2002)
Scotia Sea (57°–60°S, 52°W)	Winter–December	1.0–1.2	This study

equation was adopted, following the concepts of Poisson et al. (1993) and Bakker et al. (1997):

$$\Delta C/\Delta t = (\delta C/\delta t)_T + (\delta C/\delta t)_F + (\delta C/\delta t)_N + (\delta C/\delta t)_R, \quad (1)$$

where $\Delta C/\Delta t$ represents total $p\text{CO}_2$ change over time, which is the sum of variations due to thermodynamical changes (those related to temperature and salinity) $(\delta C/\delta t)_T$, air–sea exchange $(\delta C/\delta t)_F$, biological production, or NCP $(\delta C/\delta t)_N$, and a residual term $(\delta C/\delta t)_R$, which is mainly ascribed to the combined effects of physical mixing such as advective and diffusive transport, upwelling, and water mass variability. Since each term in Eq. (1) implicitly includes time integration from the winter maximum to the observation time in late spring, we must determine the time of the winter maximum and the concentrations of inorganic carbon and nutrients at that time. We calculated average changes in chemical parameters, physical condition, and biological production over the period. We considered the winter maximum as the time of year when sea surface temperature was the lowest and the mixed-layer was deepest. This time was followed by surface warming and consequent stratification. To determine the winter

maximum, we used sea surface temperature data from the weekly 1° latitude × 1° longitude spatial resolution optimum interpolation (OI) analysis. This analysis produced world ocean SST data from November 1981 to the present using both in situ and satellite sensor-derived data. Data were improved at high latitudes with a new sea ice algorithm (Reynolds et al., 2002; http://iridl.ldeo.columbia.edu/SOURCES/.NOAA.NCEP/.EMC/.CMB/.GLOBAL/.Reyn_SmithOIv2/.weekly/.sst/). Weekly SST around the study area was lowest during the first week of August 2001. However, according to sea-ice satellite data, sea ice covered the area at that time (http://iridl.ldeo.columbia.edu/SOURCES/.NOAA.NCEP/.EMC/.CMB.GLOBAL/.Reyn_SmithOIv2/.weekly/.sea_ice/). Thus, we set the starting day to 15 August, when there was no sea ice around the stations, and Δt was calculated from 15 August until the observations on 1 and 2 December (110 days). The total surface $p\text{CO}_2$ change (ΔC) was calculated by the difference between $p\text{CO}_2$ in surface water at the observation time and $p\text{CO}_2$ in the T_{\min} layer, as calculated in the previous section (Table 1). The ΔC values ranged from –8 to 13 μatm , and the daily change in surface water $p\text{CO}_2$ ($\Delta C/\Delta t$) ranged from –0.07 to 0.12 $\mu\text{atm day}^{-1}$ (Fig. 6). The total change in $p\text{CO}_2$ during the study period was small compared to the north–south gradient of surface water $p\text{CO}_2$.

4.2.1. Thermodynamical change

The thermodynamical change in surface $p\text{CO}_2$ was calculated from the winter $p\text{CO}_2$ values and the surface temperature difference between the observation time and the winter time (i.e., the T_{\min} layer) using the program of Lewis and Wallace (1998). The estimated maximum relative error for thermodynamical change was about ±6.7%. The thermodynamical $p\text{CO}_2$ changes from winter to spring at the WS stations decreased southward and ranged from 8.8 to 30.1 μatm (Fig. 6). This corresponded to a rate of 0.08–0.27 $\mu\text{atm day}^{-1}$. The changes were high (up to 30 μatm) at stations WS 6 and WS 7, close to the Polar and Scotia Fronts, respectively, where SST increased by 0.8–1.7 °C.

Bakker et al. (1997) reported that the thermodynamical change between 46.8°S and 59.8°S along 6°W during October–November 1992 was high at the Polar Front (0.54 $\mu\text{atm day}^{-1}$) and lower in the Southern Antarctic Circumpolar Current (0.28 $\mu\text{atm day}^{-1}$). In the Bransfield Strait, Bellingshausen Sea, and Gerlache Strait, Álvarez et al. (2002) reported thermodynamical $p\text{CO}_2$ changes from 0.03 to 0.39 $\mu\text{atm day}^{-1}$ in summer 1995/1996. In the Bellingshausen domain, which encompasses the southern boundary of the Antarctic

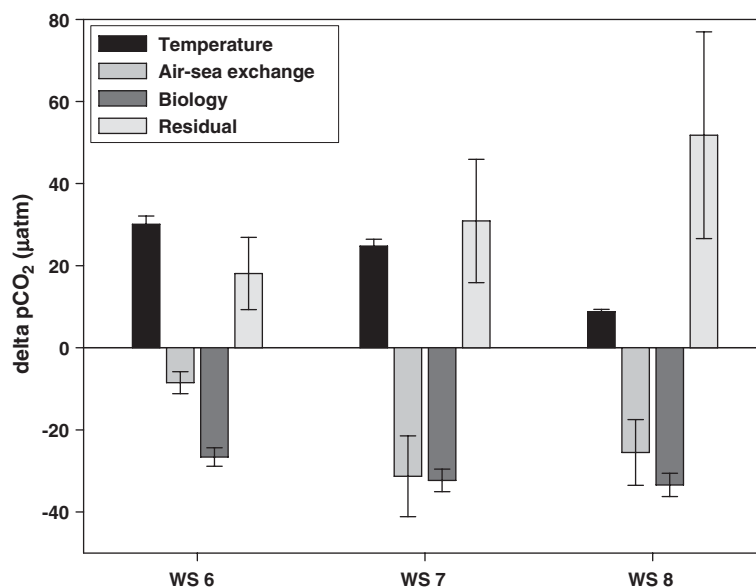


Fig. 6. The $p\text{CO}_2$ variation due to each process in the mass balance model (Eq. (1)) during the winter to observation time, plotted versus the hydrographic stations along 52°W .

Circumpolar Current, seasonal warming was the main process driving the increase in surface $p\text{CO}_2$. In contrast, in the Gerlache Strait, which is sheltered by the Antarctic Peninsula, a thermodynamical $p\text{CO}_2$ change of $0.03 \mu\text{atm day}^{-1}$ was not significant to the budget (Álvarez et al., 2002). The higher thermodynamical $p\text{CO}_2$ change in the frontal waters is due to large temperature variation in the frontal regime, not only from seasonal warming but also from meandering of the front.

4.2.2. Air–sea exchange

After sea ice retreat, CO_2 exchange between air and the sea surface should be active and affect the surface $p\text{CO}_2$. The change in surface $p\text{CO}_2$ due to air–sea exchange flux (F_{CO_2}) was estimated according to Bakker et al. (1997) as

$$(\delta C/\delta t)_F = -F_{\text{CO}_2} \beta p\text{CO}_2 \text{TDIC}^{-1},$$

where β is the buffer (or Revelle) factor, $p\text{CO}_2$ is surface water $p\text{CO}_2$, and TDIC is the total amount of DIC in the mixed layer (about 100 m depth) at the beginning of the period. The CO_2 exchange flux ($\text{mmol C m}^{-2} \text{day}^{-1}$) between the atmosphere and the ocean can be estimated (e.g., Liss and Merlivat, 1986) from

$$F_{\text{CO}_2} = ks(\Delta p\text{CO}_2),$$

where k is the gas transfer velocity (cm h^{-1}), s is the solubility of the CO_2 gas in seawater ($\text{mol kg}^{-1} \text{atm}^{-1}$;

Weiss, 1974), and $\Delta p\text{CO}_2$ is the difference between atmospheric and surface seawater $p\text{CO}_2$. Here, we used the function by Wanninkhof (1992) to calculate the gas transfer velocity ($k=0.31u^2(\text{Sc}/660)^{-0.5}$), using the wind speed (u) at 10 m above the sea surface and the Schmidt number of CO_2 (Sc), a dimensionless function of temperature and salinity. However, to evaluate $(\delta C/\delta t)_F$ from winter until the study period, time-integrated CO_2 fluxes were necessary. Historical data of surface seawater $p\text{CO}_2$ and wind speed (i.e., transfer velocity, k) were required, because these values are critical for computing time-integrated CO_2 fluxes. We used weekly wind speed data obtained by QuickSCAT, a NASA Quick Scatterometer capable of acquiring all-weather, high-resolution measurements of near-surface winds over global oceans at 2 m s^{-1} accuracy (<http://winds.jpl.nasa.gov/missions/quikscat/quikindex.html>). Weekly averaged values for $p\text{CO}_2$, TDIC, and β were also calculated using concentrations for winter and the observation time, assuming that temporal changes of those properties between the winter time and the observation time were linear with time. We further assumed that atmospheric $p\text{CO}_2$ was constant during the observation periods at $372 \mu\text{atm}$, the average value along the WS line (Fig. 3b). Relative error for this calculation, based on wind speed, thus the gas transfer velocity, was $\pm 31.4\%$.

For the WS stations, total $p\text{CO}_2$ changes caused by air–sea exchange from winter to spring ranged from -8.5 to $-31.3 \mu\text{atm}$ at rates of -0.08 to $-0.28 \mu\text{atm}$

day⁻¹ (Fig. 6). According to these results, the sea around the WS stations acted as a source of atmospheric CO₂ from winter to spring. The CO₂ air–sea fluxes at stations WS 7 and 8 were several times higher than at WS 6. The weekly averaged wind strength around the study area was relatively constant (about 9–11 m s⁻¹ from winter to spring). The winter value of *p*CO₂ determined north–south differences in the air–sea flux. Thus, the high CO₂ outgassing at stations WS 7 and 8 was ascribed to the high winter surface water *p*CO₂. A similar conclusion was reached by Álvarez et al. (2002) in the western basin of Bransfield Strait in December 1995. High *p*CO₂ was observed south of the Bransfield Front (BF), characterized by water with a Weddell Sea influence. The region north of the BF, which has water with a Bellingshausen influence, acted as a CO₂ sink. This pattern implies that regions affected by water masses from the Weddell Sea may act as CO₂ sources from winter to spring due to high mixed-layer CO₂ concentrations. Bakker et al. (1997) reported that south of the Polar Front, the sea acted as either a CO₂ source or a variable CO₂ source-sink to the atmosphere, while around the Polar Front, the sea acted as a sink due to *p*CO₂ drawdown caused by a spring bloom. Thus, whether surface seawater is a net CO₂ source or sink for the atmosphere after the retreat of sea ice in spring and early summer depends on various conditions (e.g., CO₂ concentrations in the preceding winter, surface warming, and NCP).

4.2.3. Biological change

Change in surface *p*CO₂ due to NCP was estimated as

$$(\delta C/\delta t)_N = -NCP_r \beta pCO_{2w} TDIC^{-1}$$

where NCP_r is the rate of NCP calculated from N deficits in the former section (mol m⁻² day⁻¹). At the WS stations, *p*CO₂ changes caused by NCP from winter to spring ranged from -27 to -33 μatm at rates from -0.24 to -0.30 μatm day⁻¹ (Fig. 6). The *p*CO₂ uptake tended to increase southward, coincident with the increase in Chl-*a* and carbon biomass of the microbial community (Kang et al., 2002; Hyun and Yang, 2003). However, the Chl-*a* concentration (<1 μg l⁻¹) was not high compared to that during an algal bloom (>~3 μg l⁻¹); SeaWiFS images from November and December 2001 showed no traces of a spring bloom around the study area (Yoo et al., 2002, 2003).

Along the 6°W line, during October–November 1992, the amount of NCP, and thus *p*CO₂ drawdown, varied in accordance with the spring bloom. Around

the Polar Front, algal blooms developed and resulted in a Chl-*a* increase and an *f*CO₂ decrease of 45.5 mmol m⁻² day⁻¹ and -1.31 μatm day⁻¹, respectively. At the same time, south of the front, Chl-*a* and *f*CO₂ changes were very low: 0.7 mmol m⁻² day⁻¹ and -0.03 μatm day⁻¹, respectively (Bakker et al., 1997). In December 1995 and February 1996 at the Gerlache Strait, where the primary production values were high and nutrient anomalies occurred, NCP and *p*CO₂ drawdown values were 30.8 mmol m⁻² day⁻¹ and -3.5 μatm day⁻¹, respectively, but at the Bransfield Strait, where no bloom signal was detected, they were only 11.1 mmol m⁻² day⁻¹ and -1.6 μatm day⁻¹, respectively (Álvarez et al., 2002). Thus, in the Antarctic region, the values of NCP and *p*CO₂ drawdown show differences of several orders of magnitude, depending on whether a phytoplankton bloom has developed.

According to SeaWiFS images of the study area from 1997 to 2001 (Yoo et al., 2002, 2003), surface Chl-*a* showed the highest values in January and/or February and had inter-annual variation. Although the spring bloom had not developed around this study area during the study period, *p*CO₂ drawdown due to biological activity was comparable to the rise in *p*CO₂ due to seasonal warming (Fig. 6). If a bloom was to develop, *p*CO₂ drawdown would exceed the *p*CO₂ increase due to seasonal warming and would act as a significant CO₂ sink.

4.2.4. Residual change

Residual *p*CO₂ changes were obtained by subtracting thermodynamical change, air–sea change, and biological change from the observed total *p*CO₂ change. The maximum relative error for the residual term was about ±48.6%, taking into account estimated errors for the total, thermodynamical, air–sea, and biological terms. These residual *p*CO₂ changes represent the balance of the total change, which was not explained by thermodynamical, air–sea, and biological change and are mainly ascribed to physical mixing (e.g., advective and diffusive transport, upwelling, and water mass variability). At the WS stations, the residual *p*CO₂ change ranged from 18–52 μatm at rates of 0.16–0.47 μatm day⁻¹. The most remarkable trend was an increase to the south (Fig. 6). At station WS 8, the southernmost station, the residual term (i.e., physical mixing) was the main cause of surface *p*CO₂ variation and was much higher (0.47 μatm day⁻¹) than biological production. At station WS 7, the absolute effect of physical processes was comparable to that of the biological

production and air–sea exchange. In contrast, the effect of physical mixing on the surface $p\text{CO}_2$ distribution was not significant in other Antarctic regions (Bakker et al., 1997; Álvarez et al., 2002; Stoll et al., 2002). At the Polar Front along 6°W , physical mixing was about $0.8\text{--}1.0\text{ mmol m}^{-2}\text{ day}^{-1}$, which converted to a $p\text{CO}_2$ change of only $0.02\text{--}0.03\text{ }\mu\text{atm day}^{-1}$ (Bakker et al., 1997). However, these values only represent part of the total physical mixing effects and were calculated from Ekman upward transport and/or the eddy diffusion flux (de Baar et al., 1995). Therefore, $p\text{CO}_2$ change by physical mixing would have been underestimated or overestimated, since the estimate included only vertical components and not lateral components of the physical processes.

As mentioned in the Introduction, the Scotia Sea provides a pathway for Weddell Sea water moving towards the South Atlantic. The Weddell–Scotia Confluence, as a convergence of water masses from the Weddell and Scotia Seas, is characterized by influences from winter convection (Deacon, 1937; Deacon and Foster, 1977), lateral and vertical boundary mixing, injection of melt-water (Patterson and Sievers, 1980), and advection of shelf waters (Gordon and Nowlin, 1978) such as northwestern Weddell Sea shelf water (Whitworth et al., 1994; von Gyldenfeldt et al., 2002). The WS stations located in the southern part of the Scotia Sea and northern part of the Weddell–Scotia Confluence along 52°W are characterized by strong physical mixing. Physical mixing contributed importantly to total $p\text{CO}_2$ variation, as compared to other Antarctic regions. The southward increase in physical mixing in this study suggests that vertical and lateral water mass transport from the deep water and/or the Weddell Sea is an important process in surface $p\text{CO}_2$ variation, especially around the Weddell–Scotia Confluence.

5. Conclusion

The amount of biologically incorporated inorganic carbon in areas south of the Scotia Sea and in the Weddell–Scotia Confluence from winter to spring ($1.0\text{--}1.2\text{ mol C m}^{-2}$) was comparable to that in other Antarctic areas in summer. The NCP calculated from the nitrate deficit showed a similar spatial trend as distributions of Chl-*a*, microbial carbon biomass, and particulate Fe.

Thermodynamic, air–sea exchange, biological, and physical mixing processes were evaluated with respect to their effects on surface water $p\text{CO}_2$ at

each WS station from winter to spring. The relative effect of processes controlling surface $p\text{CO}_2$ differed at each station. The thermodynamical change was more significant at WS 6 and 7 with high seasonal warming. At station WS 6, seasonal warming was the main factor in surface $p\text{CO}_2$ variation. The air–sea exchange was highest at stations WS 7 and WS 8 located in the Weddell–Scotia Confluence, and the study area acted as a CO_2 source during the study period. The $p\text{CO}_2$ drawdown caused by biological production was similar among the stations compared to spatial variation in other processes and showed values that could counteract the $p\text{CO}_2$ increase by seasonal warming. Compared to other Antarctic sites, the most distinctive point in this balance was the contribution of physical mixing to the total $p\text{CO}_2$ variation. At WS 8, the station closest to the Weddell Sea, physical mixing was the main process affecting surface $p\text{CO}_2$. Physical mixing is an important factor controlling surface $p\text{CO}_2$ variation at the WS stations, due to geographical characteristics, complex topography, and proximity to the Weddell Sea. Generally, the processes were balanced at the stations during the study period because thermodynamical change and physical mixing counteracted biological production and air–sea exchange. Thus, during the study period the two former processes created a source of CO_2 to the atmosphere and the two latter processes created a CO_2 sink.

Net community production and the main controlling factors of surface $p\text{CO}_2$ along 52°W from winter to December 2001 were spatially variable. Each station had a characteristic biogeochemical environment as well as distinct physical conditions. The results found here also support the idea of the Southern Ocean as a “mosaic” of subsystems (Tréguer and Jacques, 1992; Álvarez et al., 2002; Castro et al., 2002). This area, characterized by freshly ventilated Weddell Sea water masses, requires careful study to obtain reliable annual flux estimates for the Southern Ocean.

Acknowledgements

The authors thank the officers and crew of the *R/V Yuzhmorgeologia* for their help during the cruises. We are grateful to Prof. Frank J. Millero and his group for providing our TA and $p\text{CO}_2$ systems. This research was supported by KORDI projects PP04104 and PE87000. We thank three anonymous referees for their constructive comments on the manuscript.

References

- Álvarez, M., Ríos, A.F., Rosón, G., 2002. Spatio-temporal variability of air–sea fluxes of carbon dioxide and oxygen in the Bransfield and Gerlache Straits during Austral summer 1995–96. *Deep-Sea Research II* 49, 643–662.
- Arrigo, K.R., Robinson, D.H., Worthen, D.L., Dunbar, R.B., DiTullio, G.R., VanWoert, M., Lizotte, M.P., 1999. Phytoplankton community structure and the drawdown of nutrients and CO₂ in the Southern Ocean. *Science* 283, 365–367.
- de Baar, H.J.W., Buma, A.G.J., Nolting, R.F., Cadée, G.C., Jacques, G., Tréguer, P.J., 1990. On iron limitation of the Southern Ocean: experimental observations in the Weddell and Scotia Seas. *Marine Ecology. Progress Series* 65, 105–122.
- de Baar, H.J.W., de Jong, J.T.M., Bakker, D.C.E., Löscher, B.M., Veth, C., Bathmann, U.V., Smetacek, V., 1995. Importance of iron for plankton blooms and carbon dioxide drawdown in the Southern Ocean. *Nature* 373, 412–415.
- Bakker, D.C.E., de Baar, H.J.W., Bathmann, U.V., 1997. Changes of carbon dioxide in surface waters during spring in the Southern Ocean. *Deep-Sea Research II* 44 (1–2), 91–127.
- Bates, N.R., Hansell, D.A., Carlson, C.A., Gordon, L.I., 1998. Distribution of CO₂ species, estimates of net community production and air–sea CO₂ exchange in the Ross Sea polynya. *Journal of Geophysical Research* 103, 2883–2896.
- Belkin, I.M., Gordon, A.L., 1996. Southern ocean fronts from the Greenwich meridian to Tasmania. *Journal of Geophysical Research* 101 (C2), 3675–3696.
- Bellerby, R.G.J., Turner, D.R., Robertson, J.E., 1995. Surface pH and pCO₂ distributions in the Bellingshausen Sea, Southern Ocean, during early austral summer. *Deep-Sea Research II* 42, 1093–1107.
- Bradshaw, A.L., Brewer, P.G., 1988. High precision measurements of alkalinity and total carbon dioxide in seawater by potentiometric titration: 1. Presence of unknown protolyte(s)? *Marine Chemistry* 23, 69–86.
- Carmack, E.C., 1977. Water characteristics of the Southern Ocean south of the polar front. In: Angel, M. (Ed.), *A Voyage of Discovery*. Pergamon Press, London, pp. 15–41.
- Castro, C.G., Ríos, A.F., Doval, M.D., Pérez, F.F., 2002. Nutrient utilization and chlorophyll distribution in the Atlantic sector of the Southern Ocean during Austral summer 1995–96. *Deep-Sea Research II* 49, 623–641.
- Chipman, D., Marra, J., Takahashi, T., 1993. Primary production at 47°N and 20°W in the North Atlantic Ocean: a comparison between ¹⁴C incubation method and the mixed layer carbon budget. *Deep-Sea Research I* 40, 151–169.
- Codispoti, L.A., Friederich, G.E., Hood, D.W., 1986. Variability in the inorganic carbon system over the southeastern Bering Sea shelf during spring 1980 and spring–summer 1981. *Continental Shelf Research* 5, 133–160.
- Deacon, G.E.R., 1937. The hydrology of the Southern Ocean. *Discovery Reports* 9, 1–64.
- Deacon, G.E.R., Foster, T.D., 1977. The boundary region between the Weddell Sea and Drake Passage currents. *Deep-Sea Research* 24, 505–510.
- Dickson, A.G., 1990. Standard potential of the (AgCl(s)+1.2 H₂(g) = Ag(s)+HCl(aq)) and the standard acidity constant of the ion HSO₄⁻ in synthetic seawater from 273.15 to 318.15 K. *The Journal of Chemical Thermodynamics* 22, 113–127.
- Dickson, A.G., Millero, F.J., 1987. A comparison of the equilibrium constants for the dissociation of carbonic acid in seawater media. *Deep-Sea Research* 34, 1733–1743.
- Fahrbach, E., Rohardt, G., Scheele, N., Schröder, M., Strass, V., Wisotzki, A., 1995. Formation and discharge of deep and bottom water in the northwestern Weddell Sea. *Journal of Marine Research* 53, 515–538.
- Gill, A.E., 1973. Circulation and bottom water production in the Weddell Sea. *Deep-Sea Research* 20, 111–140.
- Gordon, A.L., 1971. Antarctic polar front zone. In: Reid, J.L. (Ed.), *Antarctic Oceanology I. Antarct. Res. Ser.*, vol. 15. AGU, Washington, D.C, pp. 205–221.
- Gordon, A.L., Nowlin Jr., W.D., 1978. The basin waters of the Bransfield Strait. *Journal of Physical Oceanography* 8, 258–264.
- Gordon, A.L., Georgi, D.T., Taylor, H.W., 1977. Antarctic Polar Front Zone in the western Scotia Sea. *Journal of Physical Oceanography* 7, 309–328.
- Goyet, C., Peltzer, E.T., 1993. Comparison of the August–September 1991 and 1979 surface partial pressure of CO₂ distribution in the Equatorial Pacific Ocean near 150°W. *Marine Chemistry* 45, 257–266.
- von Gyldenfeldt, Anna-B. von, Fahrbach, E., García, M.A., Schröder, M., 2002. Flow variability at the tip of the Antarctic Peninsula. *Deep-Sea Research II* 49, 4743–4766.
- Hoppema, M., Goeyens, L., 1999. Redfield behavior of carbon, nitrogen, and phosphorus depletions in Antarctic surface water. *Limnology and Oceanography* 44 (1), 220–224.
- Hoppema, M., Fahrbach, E., Schröder, M., Wisotzki, A., de Baar, H.J.W., 1995. Winter–summer difference of carbon dioxide and oxygen in the Weddell Sea surface layer. *Marine Chemistry* 51, 177–192.
- Hoppema, M., Fahrbach, E., Richter, K.-U., de Baar, H.J.W., Kattner, G., 1998a. Enrichment of silicate and CO₂ and circulation of the bottom water in the Weddell Sea. *Deep-Sea Research I* 45, 1797–1817.
- Hoppema, M., Fahrbach, E., Stoll, M.H.C., de Baar, H.J.W., 1998b. Increase of carbon dioxide in the bottom water of the Weddell Sea, Antarctica. *Marine Chemistry* 59, 201–210.
- Hoppema, M., de Baar, H.J.W., Bellerby, R.G.J., Fahrbach, E., Bakker, K., 2002. Annual export production in the interior Weddell Gyre estimated from a chemical mass balance of nutrients. *Deep-Sea Research II* 49, 1675–1689.
- Hyun, J.-H., Yang, E.-J., 2003. Distribution and structure of the microbial community in the Weddell Sea and Bransfield Strait. *Oceanographic Studies on Antarctic Marine Living Resources and Ecosystems. BSPP 02104-00-1511-7*, pp. 241–272 (in Korean, with English Abstr.).
- IPCC, 2001. The Scientific basis. In: Houghton, J.T., Ding, Y., Griggs, D.J., Noguera, M., van der Linden, P.J., Dai, X., Maskell, K., Johnson, C.A. (Eds.), *Contribution of Working Group I to the Third Assessment Report of the Intergovernmental Panel on Climate Change*. Cambridge University Press, Cambridge, U.K.; New York, NY, USA, p. 39.
- Ishii, M., Inoue, H.Y., Matsueda, H., Tanoue, E., 1998. Close coupling between seasonal biological production and dynamics of dissolved inorganic carbon in the Indian Ocean sector and the western Pacific Ocean sector of the Antarctic Ocean. *Deep-Sea Research I* 45, 1187–1209.
- Ishii, M., Inoue, H.Y., Matsueda, H., 2002. Net community production in the marginal ice zone and its importance for the variability of the oceanic pCO₂ in the Southern Ocean south of Australia. *Deep-Sea Research II* 49, 1691–1706.

- Jennings Jr., J.C., Gordon, L.I., Nelson, D.M., 1984. Nutrient depletion indicates high primary productivity in the Weddell Sea. *Nature* 309, 51–54.
- Kang, S.-H., Kang, J.-S., Kim, E.-J., Kang, Y.-C., Kim, D., Shim, J., Yoo, S.J., Lee, J.H., Kang, D., 2002. Distribution pattern of phytoplankton in the Sub-Antarctic and the Antarctic in the western Atlantic Ocean. *Oceanographic Studies on Antarctic Marine Living Resources and Ecosystems*. BSPP 001-B4-1405-7, pp. 257–306 (in Korean, with English Abstr.).
- Karl, D.M., Tilbrook, B.D., Tien, G., 1991. Seasonal coupling of organic matter production and particle flux in the western Bransfield Strait, Antarctica. *Deep-Sea Research* 38, 1097–1126.
- Keeling, C.D., Whorf, T.P., 1994. Atmospheric CO₂ records from sites in the SIO air sampling network. In: Boden, T.A., Kaiser, D.P., Sepanski, R.J., Stoss, F.W. (Eds.), *Trends '93', A Compendium of Data on Global Change*, ORNL/CDIAC-65. Oak Ridge National Laboratory, Oak Ridge, TN, USA, pp. 16–26.
- Kim, K.T., 2003. Accurate analysis of iron in seawaters of the Weddell Sea and the polar front area (Antarctica). *Oceanographic Studies on Antarctic Marine Living Resources and Ecosystems*. BSPP 02104-00-1511-7, pp. 229–240 (in Korean, with English Abstr.).
- Knap, A., Michaels, A., Close, A., Ducklow, H., Dickson, A., 1996. Protocols for the Joint Global Ocean Flux Study (JGOFS) core measurements. JGOFS Report no.19, vi+170pp. Reprint of the IOC Manuals and Guides no.29, UNESCO.
- Lee, K., 2001. Global net community production estimated from the annual cycle of surface water total dissolved inorganic carbon. *Limnology and Oceanography* 46 (6), 1287–1297.
- Lewis, E., Wallace, D.W.R., 1998. Program Developed for CO₂ System Calculations. ORNL/CDIAC-105. Carbon Dioxide Information Analysis Center, Oak Ridge National Laboratory, US Department of Energy, Oak Ridge, TN, <http://cdiac.esd.ornl.gov/oceans/co2rprt.html>.
- Liss, P., Merlivat, L., 1986. Air–sea exchange rates: introduction and synthesis. In: Buat-Ménard, P. (Ed.), *The Role of Air–sea Exchange in Geochemical Cycling*. NATO ASI Series C., vol. 185. D. Reidel Publishing, Dordrecht, pp. 113–127.
- Louanchi, F., Najjar, R.G., 2000. A global monthly climatology of phosphate, nitrate, and silicate in the upper ocean: Spring–summer export production and shallow remineralization. *Global Biogeochemical Cycles* 14 (3), 957–977.
- Martin, J.H., Fitzwater, S.E., Gordon, R.M., 1990. Iron deficiency limits phytoplankton growth in Antarctic waters. *Global Biogeochemical Cycles* 4 (1), 5–12.
- Metzl, N., Beauverger, C., Brunet, C., Goyet, C., Poisson, A., 1991. Surface water pCO₂ in the Western Indian Sector of the Southern Ocean: a highly variable CO₂ source/sink region during the austral summer. *Marine Chemistry* 35, 85–95.
- Midorikawa, T., Umeda, T., Hiraishi, N., Ogawa, K., Nemoto, K., Kubo, N., Ishii, M., 2002. Estimation of seasonal net community production and air–sea CO₂ flux based on the carbon budget above the temperature minimum layer in the western subarctic North Pacific. *Deep-Sea Research I* 49, 339–362.
- Millero, F.J., Zhang, J.Z., Lee, K., Campbell, D.M., 1993. Titration alkalinity of seawater. *Marine Chemistry* 44 (2–4), 153–165.
- Minas, H.J., Minas, M., 1992. Net community production in “high nutrient-low chlorophyll” waters of the tropical and Antarctic Oceans: grazing vs. iron hypothesis. *Oceanologica Acta* 15 (2), 145–162.
- Minas, H.J., Minas, M., Packard, T.T., 1986. Productivity in upwelling areas deduced from hydrographic and chemical fields. *Limnology and Oceanography* 31, 1182–1206.
- Murata, A., Kumamoto, Y., Saito, C., Kawakami, H., Asanuma, I., Kusakabe, M., Inoue, H.Y., 2002. Impact of a spring phytoplankton bloom on the CO₂ systems in the mixed layer of the northwestern North Pacific. *Deep-Sea Research II* 49, 5531–5555.
- Naveira Garabato, A.C., Heywood, K.J., Stevens, D.P., 2002. Modification and pathways of Southern Ocean Deep Waters in the Scotia Sea. *Deep-Sea Research I* 49 (4), 681–705.
- Orsi, A.H., Johnson, G.C., Bullister, J.L., 1999. Circulation, mixing and production of Antarctic Bottom Water. *Progress in Oceanography* 43, 55–109.
- Patterson, S.L., Sievers, H.A., 1980. The Weddell–Scotia confluence. *Journal of Physical Oceanography* 10, 1584–1610.
- Poisson, A., Metzl, N., Brunet, C., Schauer, B., Bres, B., Ruiz-Pino, D., Louanchi, F., 1993. Variability of sources and sinks of CO₂ in the western Indian and Southern Oceans during the year 1991. *Journal of Geophysical Research* 98, 22759–22778.
- Pollard, R.T., Lucas, M.I., Read, J.F., 2002. Physical controls on biogeochemical zonation in the Southern Ocean. *Deep-Sea Research II* 49, 3289–3305.
- Pondaven, P., Ragueneau, O., Tréguer, P., Hauvespre, A., Dezileau, L., Reyss, J.L., 2000. Resolving the ‘opal paradox’ in the Southern Ocean. *Nature* 405, 168–172.
- Redfield, A.C., Ketchum, B.H., Richard, F.A., 1963. The influence of organisms on the composition of sea-water. In: Hill, M.M. (Ed.), *The Sea*, vol. 2. Interscience, New York, pp. 26–77.
- Reynolds, R.W., Rayner, N.A., Smith, T.M., Stokes, D.C., Wang, W., 2002. An improved in situ and satellite SST analysis for climate. *Journal of Climate* 15 (13), 1609–1625.
- Robertson, J.E., Watson, A.J., 1993. Estimation of primary production by observation of changes in the mesoscale carbon dioxide field. *ICES Marine Science Symposia* 197, 207–214.
- Robertson, J.E., Watson, A.J., 1995. A summer-time sink for atmospheric carbon dioxide in the Southern Ocean between 88°W and 80°E. *Deep-Sea Research II* 42 (4–5), 1081–1091.
- Roy, R.N., Roy, L.N., Vogel, K.M., Porter-Moore, C., Pearson, T., Good, C.E., Millero, F.J., Campbell, D.M., 1993. The dissociation constants of carbonic acid in seawater at salinities 5 to 45 and temperatures 0 to 45 °C. *Marine Chemistry* 44, 249–267.
- Rubin, S.I., Takahashi, T., Chipman, D.W., Goddard, J.G., 1998. Primary productivity and nutrient utilization ratios in the Pacific sector of the Southern Ocean based on seasonal changes in seawater chemistry. *Deep-Sea Research I* 45, 1211–1234.
- Sarmiento, J.L., 1993. Atmospheric CO₂ stalled. *Nature* 365, 697–698.
- Sarmiento, J.L., Orr, J.C., Siegenthaler, U., 1992. A perturbation simulation of CO₂ uptake in an ocean general circulation model. *Journal of Geophysical Research* 97C, 3621–3645.
- Stoll, M.H.C., Thomas, H., De Baar, H.J.W., Zondervan, I., De Jong, E., Bathmann, U.V., Fahrbach, E., 2002. Biological versus physical processes as drivers of large oscillations of the air–sea CO₂ flux in the Antarctic marginal ice zone during summer. *Deep-Sea Research I* 49, 1651–1667.
- Sweeney, C., Hansell, D.A., Carlson, C.A., Codispoti, L.A., Gordon, L.I., Marra, J., Millero, F.J., Smith, W.O., Takahashi, T., 2000a. Biogeochemical regimes, net community production and carbon export in the Ross Sea, Antarctica. *Deep-Sea Research II* 47, 3369–3394.
- Sweeney, C., Smith, W.O., Hales, B., Bidigare, R.R., Carlson, C.A., Codispoti, L.A., Gordon, L.I., Hansell, D.A., Millero, F.J., Park, M.-O., Takahashi, T., 2000b. Nutrient and carbon removal ratios and fluxes in the Ross Sea, Antarctica. *Deep-Sea Research II* 47, 3395–3421.

- Takahashi, T., Olafsson, J., Goddard, J.G., Chipman, D.W., Sutherland, S.C., 1993. Seasonal variations of CO₂ and nutrients in the high-latitude surface oceans: a comparative study. *Global Biogeochemical Cycles* 7 (4), 843–878.
- Takahashi, T., Sutherland, S.C., Sweeny, C., Poisson, A., Metzl, N., Tilbrook, B., Nates, N., Wanninkhof, R., Feely, R.A., Sabine, C., Olafsson, J., Nojiri, Y., 2002. Global sea–air CO₂ flux based on climatological surface ocean pCO₂ and seasonal biological and temperature effects. *Deep-Sea Research II* 49, 1601–1622.
- Tans, P.P., Fung, I.Y., Takahashi, T., 1990. Observational constraints on the global atmospheric CO₂ budget. *Science* 247, 1431–1438.
- Tréguer, P., Jacques, G., 1992. Dynamics of nutrients and phytoplankton, and fluxes of carbon, nitrogen and silicon in the Antarctic Ocean. *Polar Biology* 12, 149–162.
- Tsurushima, N., Nojiri, Y., Imai, K., Watanabe, S., 2002. Seasonal variations of carbon dioxide system and nutrients in the surface mixed layer at station KNOT (44N, 155°E) in the subarctic western North Pacific. *Deep-Sea Research II* 49, 5377–5394.
- Wanninkhof, R., 1992. Relationship between wind speed and gas exchange over the ocean. *Journal of Geophysical Research* 97, 7373–7382.
- Wanninkhof, R., Thoning, K., 1993. Measurement of fugacity of CO₂ in surface water using continuous and discrete sampling methods. *Marine Chemistry* 44, 189–204.
- Weiss, R.F., 1970. The solubility of nitrogen, oxygen and argon in water and seawater. *Deep-Sea Research I* 17, 721–735.
- Weiss, R.F., 1974. Carbon dioxide in water and seawater: the solubility of a non-ideal gas. *Marine Chemistry* 2, 203–205.
- Weiss, R., 1981. Determinations of carbon dioxide and methane by dual catalytic flame ionization chromatography and nitrous oxide by electron capture chromatography. *Journal of Chemical Science* 19, 61–616.
- Weiss, R.F., Östlund, H.G., Craig, H., 1979. Geochemical studies of the Weddell Sea. *Deep-Sea Research* 26, 1093–1120.
- Whitworth III, T., Nowlin Jr., W.D., Orsi, A.H., Locarnini, R.A., Smith, S.G., 1994. Weddell Sea Shelf Water in the Bransfield Strait and Weddell–Scotia Confluence. *Deep-Sea Research I* 41 (4), 629–641.
- Yoo, S., Park, J., Kim, H.-C., 2002. Satellite imagery of chlorophyll in the Antarctic Ocean. *Oceanographic Studies on Antarctic Marine Living Resources and Ecosystems*. BSPP 001-B4-1405-7, pp. 307–327 (in Korean, with English Abstr.).
- Yoo, S., Park, J., Kim, H.-C., 2003. Validation of SeaWiFS standard algorithm and evaluation of primary productivity in surroundings of the Drake Passage. *Oceanographic Studies on Antarctic Marine Living Resources and Ecosystems*. BSPP 02104-00-1511-7, pp. 211–228 (in Korean, with English Abstr.).